

Electrogeneration of Oxidized Corrole Dimers. Electrochemistry of (OEC)M Where M = Mn, Co, Ni, or Cu and OEC Is the Trianion of 2,3,7,8,12,13,17,18-Octaethylcorrole

Karl M. Kadish,^{*,†} Victor A. Adamian,[†] Eric Van Caemelbecke,[†] Elena Gueletii,[†] Stefan Will,[‡] Christoph Erben,[‡] and Emanuel Vogel^{*,‡}

Contribution from the Department of Chemistry, University of Houston, Houston, Texas 77204-5641, and Institut für Organische Chemie, Universität zu Köln, Greinstrasse 4, 50939 Köln, Germany

Received April 24, 1998

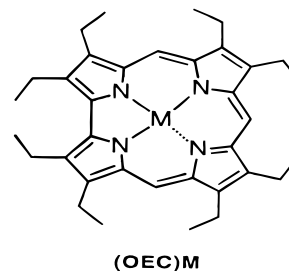
Abstract: The electrochemistry of (OEC)M where M = Mn, Co, Ni, or Cu and OEC is the trianion of 2,3,7,8,12,13,17,18-octaethylcorrole was investigated in dichloromethane, benzonitrile, or pyridine, and the oxidized compounds were characterized by UV–visible and/or ESR spectroscopy. The first two oxidations of the Co, Ni, and Cu corroles involve the reversible stepwise abstraction of 1.0 electron per two (OEC)M units and lead to [(OEC)M]₂⁺ and [(OEC)M]₂²⁺, which are assigned as π – π dimers containing oxidized corrole macrocycles and divalent central-metal ions on the basis of the electrochemical and spectroscopic data. The ESR spectrum of [(OEC)Cu]₂⁺ suggests the presence of one ESR-active Cu(II) center in the singly oxidized dimer. Further bulk electrooxidation of [(OEC)Cu]₂⁺ at potentials positive of the second oxidation results in the abstraction of a second electron from the dimeric unit and leads to a triplet ESR spectrum typical of a copper(II) dimer, from which a Cu–Cu distance of 3.88 Å is calculated. The ESR spectrum of [(OEC)Co]₂⁺ in frozen CH₂Cl₂ at 77 K has a major line at $g_{\perp} = 2.40$ with a weak signal at $g_{\parallel} = 1.89$ and is typical of a Co(II) ion. The doubly oxidized dimer, [(OEC)Co]₂²⁺, is ESR silent in CH₂Cl₂ or PhCN, thus suggesting that the two unpaired electrons of the two Co(II) ions in [(OEC)Co]₂²⁺ are coupled. The absolute potential difference between $E_{1/2}$ for generation of [(OEC)M]₂⁺ and [(OEC)M]₂²⁺ can be related to the degree of interaction between the two (OEC)M units of the dimer and follows the order Co ($\Delta E_{1/2} = 460$ mV) > Ni ($\Delta E_{1/2} = 260$ mV) > Cu ($\Delta E_{1/2} = 140$ mV). No evidence is seen for dimerization of (OEC)Mn after oxidation to its Mn(IV) form in the first electron-transfer step, and the occurrence of this metal-centered reaction may be the reason for the absence of dimerization.

Introduction

Metalloporphyrins have been synthesized with a number of different metal ions,^{1–3} with the most often characterized compounds being the cobalt(III)^{1–12} and chemically^{6,8} or electrochemically^{4,6} generated cobalt(II) derivatives. A one-electron oxidation of cobalt(III) tetraethyltetramethylcorrole was briefly mentioned by Johnson and co-workers⁴ in 1973, but it

was not until 20 years later that cobalt(III) corroles were shown to undergo three¹¹ or four¹² reversible one-electron oxidations, the first of which was proposed to generate a high-oxidation-state Co(IV) complex.¹² The electrochemical properties of cobalt(III) corroles are thus quite different from those of Co(III) porphyrins where a maximum of two one-electron oxidations can be observed,¹³ both of which occur at the macrocycle.

This paper examines the electrochemical and spectroscopic properties of neutral and oxidized (OEC)M where OEC is the trianion of 2,3,7,8,12,13,17,18-octaethylcorrole and M = Mn, Co, Ni, or Cu.



The (OEC)Ni derivative has been described¹⁴ as a Ni(II) corrole π cation radical, i.e., (OEC⁺)Ni^{II}, while (OEC)Cu has been described as a Cu(III) corrole existing in equilibrium with a Cu(II) corrole π cation radical (see eq 1), the Cu(III) form being predominant at room temperature.

[†] University of Houston.

[‡] Universität zu Köln.

(1) Johnson, A. W. *Pure Appl. Chem.* **1970**, *23*, 375.

(2) (a) Genokhova, N. S.; Melent'eva, T. A.; Berezovskii, V. M. *Russ. Chem. Rev. (Engl. Transl.)* **1980**, *49*, 1056. (b) Melent'eva, T. A. *Russ. Chem. Rev. (Engl. Transl.)* **1983**, *52*, 641.

(3) Licocchia, S.; Paolesse, R. *Struct. Bonding* **1995**, *84*, 71.

(4) Conlon, M.; Johnson, A. W.; Overend, W. R.; Rajapaksa, D.; Elson, C. M. *J. Chem. Soc., Perkin Trans. 1* **1973**, 2281.

(5) Hush, N. S.; Dyke, J. M. *J. Inorg. Nucl. Chem.* **1973**, *35*, 4341.

(6) (a) Hush, N. S.; Woolsey, I. S. *J. Chem. Soc., Dalton Trans.* **1974**, 24. (b) Hush, N. S.; Dyke, J. M.; Williams, M. L.; Woolsey, I. S. *J. Chem. Soc., Dalton Trans.* **1974**, 395.

(7) Murakami, Y.; Yamada, S.; Matsuda, Y.; Sakata, K. *Bull. Chem. Soc. Jpn.* **1978**, *51*, 123.

(8) Murakami, Y.; Matsuda, Y.; Sakata, K.; Yamada, S.; Tanaka, Y.; Aoyama, Y. *Bull. Chem. Soc. Jpn.* **1981**, *54*, 163.

(9) Paolesse, R.; Licocchia, S.; Fanciullo, M.; Morgante, E.; Boschi, T. *Inorg. Chim. Acta* **1993**, *203*, 107.

(10) Paolesse, R.; Licocchia, S.; Bandoli, G.; Dolmella, A.; Boschi, T. *Inorg. Chem.* **1994**, *33*, 1171.

(11) Kadish, K. M.; Koh, W.; Tagliatesta, P.; Sazou, D.; Paolesse, R.; Licocchia, S.; Boschi, T. *Inorg. Chem.* **1992**, *31*, 2305.

(12) Adamian, V. A.; D'Souza, F.; Licocchia, S.; Di Vona, M. L.; Tassoni, E.; Paolesse, R.; Boschi, T.; Kadish, K. M. *Inorg. Chem.* **1995**, *34*, 532.



Similar assignments have been made for a related manganese octamethylcorrole, (OMC)Mn, which was described as a Mn(III) species in the solid state but as a Mn(II) corrole π cation radical in solution containing noncoordinated solvents.¹⁵ However, virtually nothing is known about the electrooxidized forms of these compounds, which are the main focus of this paper. As will be demonstrated, the investigated Cu, Ni, and Co corroles are converted upon oxidation from monomeric species which contain a formal metal(III) ion to dimeric species of the type $[(\text{OEC})\text{M}]_2^+$ and $[(\text{OEC})\text{M}]_2^{2+}$. Both oxidized dimers are characterized as containing a metal(II) ion by UV-visible and ESR spectroscopy. This behavior contrasts with that of (OEC)-Mn, which is converted to its Mn(IV) form upon oxidation and shows no evidence for dimerization.

Experimental Section

Instrumentation. ¹H NMR spectra were recorded on a Bruker AP 300 NMR spectrometer at 300 MHz. ESR spectra were recorded on an IBM ER 100D or a Bruker ESP 380E spectrometer. The *g* values were measured with respect to diphenylpicrylhydrazyl (*g* = 2.0036 ± 0.0003). Magnetic susceptibility was measured on powder samples using a Faraday balance. Data were corrected for diamagnetism, χ_{dia} , using a value of -300×10^{-6} cgsu. Mass spectra were obtained using a Finnigan MAT 212. Elemental analysis was provided by Bayer AG (Leverkusen, Germany).

Cyclic voltammetry was carried out with an EG&G model 173 potentiostat or an IBM model EC 225 voltammetric analyzer. A three-electrode system was used and consisted of a glassy carbon or platinum disk working electrode, a platinum wire counter electrode, and a saturated calomel electrode (SCE) as the reference electrode. The SCE was separated from the bulk of the solution by a fritted-glass bridge of low porosity which contained the solvent/supporting electrolyte mixture. Variable-temperature measurements were taken in a nonisothermal electrochemical cell that was immersed in an acetone/dry ice bath which had the indicated temperature. The reference electrode was maintained at room temperature throughout the experiments and was separated from the cooled solution by a fritted bridge that contained the same solvent and supporting electrolyte as the bulk of the solution. The temperature of the solution was recorded with a thermometer (±1 °C). All potentials are referenced to the SCE. UV-visible spectroelectrochemical experiments were carried out with a Hewlett-Packard model 8452A diode array spectrophotometer. UV-visible spectra were recorded on a Perkin-Elmer Lambda 7 spectrophotometer, while IR measurements were performed with a Perkin-Elmer IR 283 or a Perkin-Elmer Series 1600 spectrometer.

Chemicals. Benzonitrile (PhCN) was purchased from Aldrich and distilled over P₂O₅ under vacuum prior to use. Absolute dichloromethane (CH₂Cl₂) and anhydrous, argon-packed *N,N*-dimethylformamide, DMF, were purchased from Aldrich and used without further purification. Pyridine (py), received from Aldrich, was distilled over CaH₂ under nitrogen. CDCl₃, used for NMR measurements, was obtained from Aldrich and used as received. Tetra-*n*-butylammonium perchlorate was purchased from Sigma, recrystallized from ethyl alcohol, and dried under vacuum at 40 °C for at least 1 week prior to use.

Synthesis of (OEC)Cu and (OEC)Ni. The Cu and Ni derivatives were synthesized according to literature procedures.¹⁴

Synthesis of (OEC)Mn. A solution of 523 mg (1 mmol) of 2,3,7,8-, 12,13,17,18-octaethylcorrole and 1.2 g (3 mmol) of Mn₂(CO)₁₀ in 30

mL of toluene was refluxed under argon for 6 h. The solvent was evaporated in a vacuum, and the residue was passed through a column of alumina using 2:1 ether/toluene as eluent. After crystallization from 2:1 toluene/hexane, (OEC)Mn was obtained as small black needles: yield 413 mg (72%); mp >300 °C. ¹H NMR (300 MHz, toluene-*d*₈), δ (ppm): 93 (singlet, 2H, H-5,15), 72 (singlet, 4H, CH₂), 68 (singlet, 1H, H-10), 40 (singlet, 4H, CH₂), 19 (singlet, 4H, CH₂), 4.3 (singlet, 4H, CH₂), 3.2 (singlet, 24H, CH₃). The assignment of the meso protons H-5,10,15 was made by comparison with a meso-*d*₃ (OEC)Mn. MS (FAB/NBA), *m/z* (%): 574 [M]⁺⁺ (100). IR (CsI), ν (cm⁻¹): 2951, 2927, 2866, 1475, 1446, 1369, 1289, 1260, 1188, 1150, 1055, 1025, 1006, 959, 884, 814, 802, 768. UV-vis (CH₂Cl₂) [λ_{max} , nm (ϵ , mol⁻¹ L cm⁻¹): 370 (48 300) sh, 390 (62 700), 480 (12 300), 590 (16 700), 730 (1300), 840 (1800). Anal. Calcd for C₃₅H₄₃N₄Mn: C, 73.15; H, 7.54; N, 9.75. Found: C, 72.95; H, 7.30; N, 9.72.

Synthesis of (OEC)Co. (2,3,7,8,12,13,17,18-Octaethylcorolato)-cobalt(III), (OEC)Co, was synthesized according to a literature procedure⁷ but with the modification that the free-base corrole was used instead of 1,19-dideoxyoctaethylbiladiene-*ac*. At 80 °C, a 20 mL DMF solution containing 625 mg (2.5 mmol) of cobalt(II) acetate tetrahydrate was added to an 80 mL DMF solution containing 523 mg (1 mmol) of octaethylcorrole. After 5 min, the temperature of the mixture was lowered to 4 °C and held at this temperature for 2 h. The precipitated cobalt corrole, (OEC)Co, was isolated by filtration and thoroughly washed with methanol. After crystallization from a mixture of methanol and chloroform, 450 mg (78%) of (OEC)Co was obtained as black needles. The compound started decomposing above 170 °C. ¹H NMR (CDCl₃, 300 MHz), δ (ppm): 154.2 (singlet, 4H, CH₂), 74.5 (singlet, 4H, CH₂), 33.0 (singlet, 2H, H-5,15), 18.5 (singlet, 4H, CH₂), 18.2 (singlet, 6H, CH₃), 10.5 (singlet, 6H, CH₃), 4.3 (singlet, 6H, CH₃), 1.4 (singlet, 6H, CH₃), -4.6 (singlet, 4H, CH₂), -21.6 (singlet, 1H, H-10). MS (EI, 70 eV), *m/z* (%): 578 (100) M⁺, 563 (12) [M - CH₃]⁺, 550 (19) [M - C₂H₄]⁺, 548 (18) [M - 2CH₃]⁺, 289 (9) M²⁺. UV-vis (CH₂Cl₂) [λ_{max} , nm (ϵ , mol⁻¹ L cm⁻¹): 258 (17 500) sh, 311 (16 700), 366 (57 300) sh, 383 (119 000), 485 (12 900) sh, 502 (13 600), 626 (2300) sh, 647 (2900), 677 (2600), 739 (1200). IR (CsI), (cm⁻¹): ν = 2962, 2929, 2869, 1480, 1449, 1369, 1055, 1016, 957, 808. μ_{eff} = 3.20 μ_{B} (293 K), μ_{eff} = 2.98 μ_{B} (81 K).

Results and Discussion

Characterization of Neutral (OEC)Co. All five- and six-coordinate Co(III) corroles and Co(III) porphyrins have previously been characterized as containing a low-spin (*S* = 0) central metal ion.¹⁻¹² This is in contrast to (OEC)Co which, in the solid state, possesses an effective magnetic moment of 3.20 μ_{B} over the temperature range 80–293 K, thus indicating an intermediate-spin (*S* = 1) cobalt(III) ion. Such a spin state is characteristic of d⁶ ions in a square planar coordination environment^{16,17} and has not been reported for any other cobalt(III) tetrapyrrole.

The ¹H NMR spectra of (OEC)Co in weakly coordinating solvents is also characteristic of an *S* = 1 spin state. The NMR spectrum is well-resolved in CDCl₃ and shows strong paramagnetic shifts with respect to resonances of low-spin cobalt(III) corroles^{3,7-12} or porphyrins.¹³ The meso protons of (OEC)Co are seen as singlets at 33.0 (H-5,15) and -21.6 ppm (H-10) while the protons of the ethyl groups are characterized by eight resonances between 154.2 and -4.6 ppm.

The paramagnetic shifts of the (OEC)Co proton resonances can be compared to shifts seen in the NMR spectra of isoelectronic iron(II) porphyrins¹⁷ and cobalt(III) tetraamide complexes¹⁶ which have a d⁶ *S* = 1 central metal ion. There is

(13) (a) Scheer, H.; Katz, J. J. In *Porphyrins and Metalloporphyrins*; Smith, K. M., Ed.; Elsevier: Amsterdam, 1975; p 399. (b) Bonnett, R.; Dimsdale, M. J. *J. Chem. Soc., Perkin Trans. 1* **1972**, 2540.

(14) Will, S.; Lex, J.; Vogel, E.; Schmickler, H.; Gisselbrecht, J.-P.; Hauptmann, C.; Bernard, M.; Gross, M. *Angew. Chem., Int. Ed. Engl.* **1997**, *36*, 357; *Angew. Chem.* **1997**, *109*, 367.

(15) Licocchia, S.; Morgante, E.; Paolesse, R.; Polizio, F.; Senge, M. O.; Tondello, E.; Boschi, T. *Inorg. Chem.* **1997**, *36*, 1564.

(16) (a) Brewer, J. C.; Collins, T. J.; Smith, M. R.; Santarsiero, B. D. *J. Am. Chem. Soc.* **1988**, *110*, 423. (b) Collins, T. J.; Richmond, T. G.; Santarsiero, B. D.; Treco, B. G. R. T. *J. Am. Chem. Soc.* **1986**, *108*, 2088.

(17) Goff, H.; La Mar, G. N.; Reed, C. A. *J. Am. Chem. Soc.* **1977**, *99*, 3641.

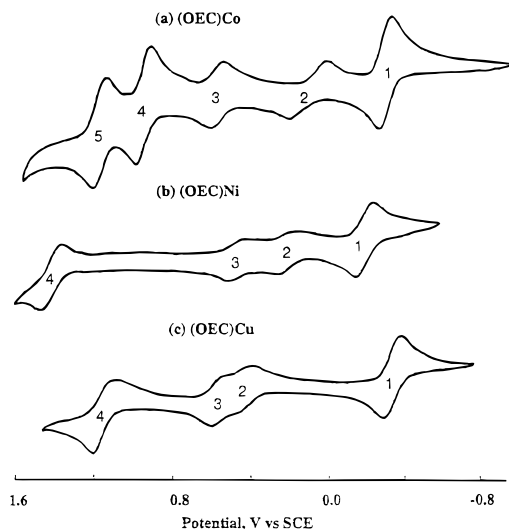


Figure 1. Continuous-scan cyclic voltammograms of (a) (OEC)Co, (b) (OEC)Ni, and (c) (OEC)Cu in CH_2Cl_2 , 0.1 M TBAP. Scan rate = 0.1 V/s. The process labeled as reaction 1 is a reduction while reactions 2–5 are oxidations of the neutral compound.

Table 1. Half-Wave Potentials, V vs SCE, and Number of Electrons Transferred^a by Bulk Electrolysis (Shown in Parentheses) per Mole of (OEC)M (M = Cu, Ni, Co, Mn) in CH_2Cl_2 , 0.1 M TBAP

M	oxidn				redn 1st
	4th	3rd	2nd	1st	
Cu		1.14 (1.0)	0.57 (0.5)	0.43 (0.5)	-0.34 (1.0)
Ni		1.41 (1.0)	0.47 (0.5)	0.21 (0.5)	-0.20 (1.0)
Co	1.17 (1.0)	0.94 (1.0)	0.57 (0.5)	0.11 (0.5)	-0.30 (1.0)
Mn ^b		1.56 (1.0)	0.93 (1.0)	0.36 (1.0)	-1.58 (1.0)

^a Coulometric values given to $\pm 10\%$. ^b $E_{1/2}$ values and coulometric data measured in PhCN.

a pronounced downfield shift of the methylene protons in (OEC)Co, consistent with a transfer of unpaired spin density from the paramagnetic Co(III) center to the π orbitals of the macrocyclic ligand (π contact shift). This suggests a $(d_{xy})^2(d_{z^2})^2(d_{xz}, d_{yz})^2$ electron configuration as has been proposed for isoelectronic $S = 1$ Fe(II) porphyrins.¹⁷ The chemical or electrochemical reduction of (OEC)Co leads to formation of a low-spin d^7 cobalt(II) corrole, [(OEC)Co]⁻, which should have a $(d_{xy})^2(d_{z^2})^2(d_{xz}, d_{yz})^3$ configuration, as was suggested for a related cobalt(II) methylethylcorrole.⁸

Murakami et al.⁷ had reported that the ¹H NMR spectrum of (OEC)Co was significantly dependent upon concentration and interpreted this result in terms of aggregation. Under our experimental conditions, the NMR spectra of (OEC)Co are independent of concentration between 10^{-3} and 10^{-1} M, which indicates the absence of aggregates for neutral (OEC)Co in solution.

Electrochemistry of (OEC)M. Two types of electrochemistry are seen for the investigated (OEC)M complexes. The first is for (OEC)Co, (OEC)Cu, and (OEC)Ni, all of which show a facile one-electron reduction and multiple oxidations with variable peak currents in simple ratios of 1:1 or 1:2 (see Figure

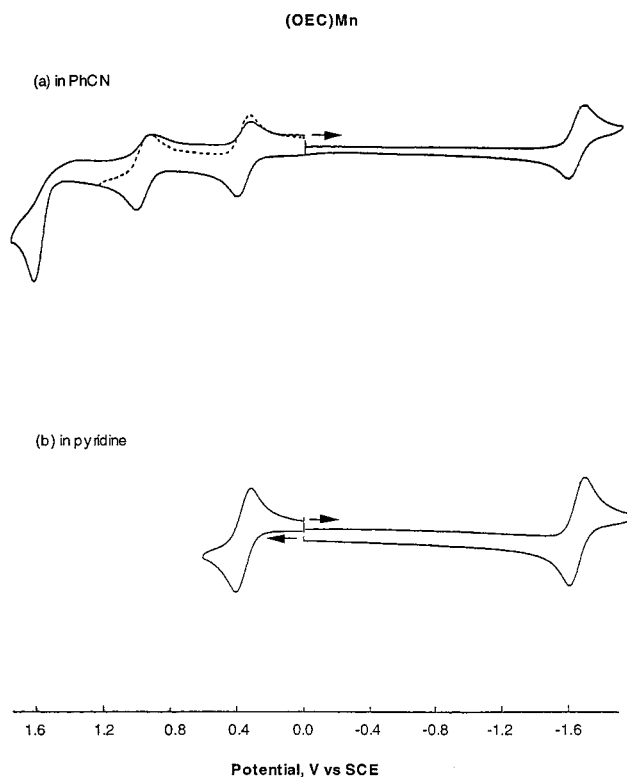


Figure 2. Cyclic voltammograms of (OEC)Mn in (a) PhCN and (b) pyridine containing 0.1 M TBAP. Scan rate = 0.1 V/s.

1 and Table 1). The second is observed only for (OEC)Mn, which is much more difficult to reduce than the other investigated (OEC)M derivatives and undergoes three well-defined oxidations, the first two of which have the same peak current as the reduction according to cyclic voltammetry (see Figure 2). The overall shape of the current–voltage curves in Figure 1 suggests the formation of electroactive dimers upon oxidation of (OEC)Co, (OEC)Ni, and (OEC)Cu, and this is indeed the case as discussed below.

Electrochemistry and ESR Spectroscopy of (OEC)Mn.

The electrochemistry of (OEC)Mn is straightforward and consistent with electrochemical data in the literature for previously investigated metallocorroles, all of which are relatively more difficult to reduce and easier to oxidize than the well-studied octaethyl- or tetraphenylporphyrins containing the same metal ion.^{11,12,18} The (OEC)Mn derivative undergoes a single one-electron reduction at $E_{1/2} = -1.58$ V and three one-electron oxidations which are located at $E_{1/2} = 0.36$, 0.93 and $E_{pa} = 1.56$ V (at a scan rate of 0.1 V/s) in PhCN, 0.1 M TBAP. Similar electrochemical behavior is seen in DMF (not shown) or pyridine (Figure 2), where the resulting (OEC)Mn(py) complex undergoes reversible one-electron-transfer reactions at $E_{1/2} = -1.58$ and 0.32 V.

The first oxidation of (OEC)Mn unambiguously leads to a Mn(IV) complex as ascertained by the ESR spectrum of the singly oxidized product obtained at 120 K in DMF. This spectrum shows a signal centered at $g_{\perp} = 3.8$ with a six-line hyperfine splitting of ~ 70 G due to the ⁵⁵Mn nucleus. A signal at $g_{\parallel} \sim 2$ was too weak to be definitively resolved. The ESR spectrum of [(OEC)Mn(DMF)]⁺ is similar to reported spectra of manganese(IV) tetraphenylporphyrin derivatives which have major components at $g_{\perp} = 3.9$ –4.5 and $a_{\perp} = 60$ –80 G.¹⁹ Hence, the one-electron-oxidation product of (OEC)Mn(DMF) can best be described as a monomeric manganese(IV) corrole, [(OEC)Mn^{IV}(DMF)]⁺, on the basis of its ESR characteristics.

(18) (a) Van Caemelbecke, E.; Will, S.; Autret, M.; Adamian, V. A.; Lex, J.; Gisselbrecht, J.-P.; Gross, M.; Vogel, E.; Kadish, K. M. *Inorg. Chem.* **1996**, *35*, 184. (b) Autret, M.; Will, S.; Van Caemelbecke, E.; Lex, J.; Gisselbrecht, J.-P.; Gross, M.; Vogel, E.; Kadish, K. M. *J. Am. Chem. Soc.* **1994**, *116*, 9141. (c) Murakami, Y.; Matsuda, Y.; Yamada, S. *J. Chem. Soc., Dalton Trans.* **1981**, 855. (d) Matsuda, Y.; Yamada, S.; Murakami, Y. *Inorg. Chem.* **1981**, 2239. (e) Murakami, Y.; Matsuda, Y.; Yamada, S. *Chem. Lett.* **1977**, 689.

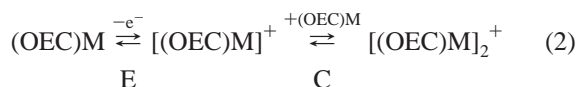
Electrochemistry of (OEC)M Where M = Cu, Co, or Ni.

The oxidations and reductions of each (OEC)M derivative are all reversible to quasireversible in CH₂Cl₂ at room temperature, as illustrated by the continuous-scan cyclic voltammograms in Figure 1. The anodic to cathodic peak separations range from 60 to 70 mV for each electrode process at room temperature except for the first oxidation of (OEC)Co, which has an $E_{pa} - E_{pc}$ of about 120 mV for a scan rate of 0.1 V/s. The anodic and cathodic peak currents for the first reduction (process 1) and third or fourth oxidation (process 4 or 5) are equal to each other, and these are approximately double those of the first and second oxidations (processes 2 and 3) under the same experimental conditions. Voltammograms similar to those in Figure 1 were obtained using single or multiple scans starting at -0.1 V and sweeping the potential in either a positive or negative direction. Similar voltammograms were also obtained in PhCN although, in this solvent, the fourth oxidation of (OEC)Co is irreversible.

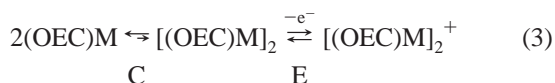
Exhaustive controlled-potential electrolysis was carried out for each electrode reaction of (OEC)M in PhCN, 0.2 M TBAP and shows that 0.5 ± 0.05 electrons are abstracted per each (OEC)M molecule in oxidation processes 2 and 3 while 1.0 ± 0.1 electrons are added or abstracted for each one molecule of (OEC)M in the redox reactions labeled as processes 1 and 4. The coulometric data are self-consistent with the ratio of peak currents in the cyclic voltammograms and can be explained by formation of oxidized dimers, namely [(OEC)M]₂⁺ after the first oxidation and [(OEC)M]₂²⁺ after the second. Electron distribution in the oxidized dimers is discussed in following sections.

A dimerization of oxidized metallocorroles has not previously been observed in solution, in part, because most previous solution studies of these metallocorroles have been carried out in strongly coordinating solvents or with corroles which contained strongly coordinating axial ligand(s)^{11,12,18} and, in part, because some of the previous studies involved derivatives with bulky substituents on the corrole macrocycle,¹² which precluded the formation of dimers.

Suggested Mechanism for Dimer Formation. Two possible mechanisms can be presented to account for the presence of [(OEC)M]₂⁺ or [(OEC)M]₂²⁺ dimers after the coulometric global abstraction of 0.5 or 1.0 electron per (OEC)M unit. The first is an electrochemical EC mechanism which would require an initial formation of [(OEC)M]⁺ followed by reaction with unoxidized (OEC)M to give [(OEC)M]₂⁺ as shown in eq 2. The



second is an electrochemical CE mechanism where a neutral [(OEC)M]₂ dimer is formed in an initial chemical step (the C step in eq 3) *prior* to oxidation, with the driving force for its formation being the *application of a positive potential*. The



proposed CE mechanism in eq 3 can occur only if two conditions are met. The first is that dimeric [(OEC)M]₂ be easier to oxidize than monomeric (OEC)M and the second is that the formation of neutral [(OEC)M]₂ be thermodynamically unfavorable *in the absence of an applied potential*. Under these

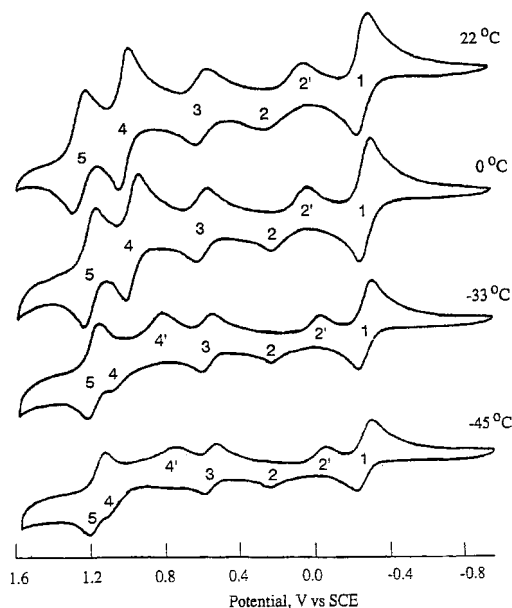
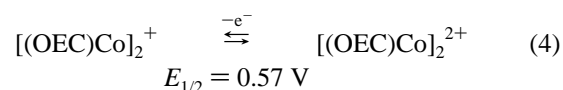


Figure 3. Continuous-scan cyclic voltammograms of (OEC)Co in CH₂Cl₂ containing 0.2 M TBAP at temperatures between +22 and -45 °C. Scan rate = 0.1 V/s.

two conditions, the difference in potential between oxidation of monomeric (OEC)M and dimeric [(OEC)M]₂ would be the driving force leading to an electrochemically induced shift of the chemical step in eq 3 toward the right as [(OEC)M]₂⁺ is formed *under the application of a positive (oxidizing) potential*. The initial solution can therefore contain almost exclusively monomeric (OEC)M (as actually indicated by the spectroscopic data) but still be oxidized via the more thermodynamically favorable process involving [(OEC)M]₂ as long as the rate of conversion between the monomeric and dimeric forms of the neutral corrole (the C step in eq 3) is sufficiently fast on the electrochemical time scale.

To ascertain which of the two mechanisms is the more probable, a series of variable-temperature experiments were carried out with (OEC)Co. A lowering of the solution temperature from +22 to -45 °C should slow the proposed dimerization reaction in eq 3, and this would be accompanied by a positive shift of the peak potential for the first oxidation.²⁰ This is indeed what is experimentally observed. In addition, the variable-temperature voltammograms shown in Figure 3 clearly rule out an EC type mechanism (eq 2) since this mechanism should lead to a well-defined and reversible one-electron oxidation (process 2) at low temperatures where the chemical step following electron transfer should not be observed due to slow kinetics.²⁰

The second oxidation of (OEC)Co (process 3 in Figures 1 and 3) is unaffected by changes in solution temperature between +22 and -45 °C, and this electrode reaction is assigned to a reversible one-electron process involving the singly and doubly oxidized corrole dimer (eq 4). The singly and doubly oxidized



cobalt dimers are sufficiently stable in PhCN to be spectroscopically characterized (see following sections), but this is not the case after the third electrooxidation (process 4), which also seems to be associated with an electrochemical CE mechanism.

(19) (a) Konishi, S.; Hoshino, M.; Imamura, M. *J. Phys. Chem.* **1982**, *86*, 4537. (b) Maliyachel, A. C.; Otvos, J. W.; Calvin, M.; Spreer, L. O. *Inorg. Chem.* **1987**, *26*, 4133.

(20) Nicholson, R. S.; Shain, I. *Anal. Chem.* **1964**, *36*, 706.

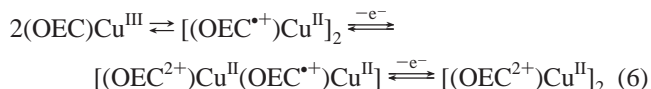
of a Cu(II) ion, which indicates that the first reduction of the formal (OEC)Cu^{III} complex results in formation of [(OEC)Cu^{II}]⁻.³²

The ESR spectrum of [(OEC)Cu]₂⁺ generated after the first oxidation is shown in Figure 5b. The signal is centered at $g_{\perp} = 2.017$ and $g_{\parallel} = 2.113$ and shows a four-line hyperfine splitting due to $I = 3/2$ Cu nuclei ($a_{\perp}^{\text{Cu}} = 196$ G) as well as a nine-line superhyperfine splitting from the four corrole nitrogens in the high-field part of the spectrum ($a_{\text{N}} = 3.3$ G). The shape of this spectrum is identical to that of the spectrum of [(OEC)Cu^{II}]⁻ (Figure 5a), clearly suggesting the existence of one ESR-active Cu(II) center in the singly oxidized dimer.

Further bulk electrooxidation of [(OEC)Cu]₂⁺ at potentials positive of the second oxidation results in abstraction of a second electron from the dimeric (OEC)Cu unit and leads to the spectrum shown in Figure 5c. The spectrum is a triplet which is centered at $g = 2.048$ and assigned to [(OEC)Cu]₂²⁺. Satellite peaks are seen in the low-field part of the spectrum while the high-field part of the spectrum is not well-resolved. The triplet nature of the spectrum is further proven by a weak half-field signal at $g = 4.21$. Both the half-peak and satellite signals show seven-line splitting from two $I = 3/2$ ⁶³Cu and ⁶⁵Cu nuclei with $a_{\text{Cu}} = 122$ G. The triplet spectrum shown in Figure 5c is typical of copper(II) dimers.³³ The distance between the two Cu(II) ions of [(OEC)Cu]₂²⁺ can be estimated from the triplet ESR spectrum in Figure 5c as 3.88 Å using equations presented in the literature.^{26,33} This is slightly larger than the 3.37 Å for the M–M distance of half-oxidized [(OEP)Cu]₂⁺ in the solid state.^{23b}

The three ESR spectra in Figure 5 confirm the dimeric structure of oxidized (OEC)Cu and also clearly indicate that the singly oxidized dimer, [(OEC)Cu]₂⁺, contains one ESR-active Cu(II) ion while the doubly oxidized dimer, [(OEC)

Cu]₂²⁺, contains two Cu(II) ions. The seemingly strange appearance of a Cu(II) central metal after oxidation of the formally copper(III) corrole can be explained by the fact that dimeric macrocycles with strong π – π interactions form common π systems which are significantly easier to oxidize than related monomeric systems with the same macrocycle.²⁴ Therefore, while monomeric (OEC)Cu contains a formal Cu(III) ion, the interaction of the two (OEC)Cu units, either before or after oxidation, may result in an internal electron transfer producing a species which contains two Cu(II) ions and one or two oxidized π ring systems (see eq 6). The dimerization of (OEC)Cu is proposed to occur prior to the electron transfer as illustrated in eq 3, and the following electron-transfer reactions would then occur as shown in eq 6 where the product of the



first oxidation is assigned on the basis of its ESR spectrum as a dimeric (OEC)Cu complex containing two Cu(II) ions, one OEC dication, OEC²⁺, and one OEC π cation radical, OEC^{•+}.

The singly oxidized Cu(II) dimer, [(OEC²⁺)Cu^{II}(OEC^{•+})Cu^{II}], may exist in either an $S = 1/2$ or an $S = 3/2$ configuration depending upon the interaction between the three unpaired electrons in the complex. The spectrum in Figure 5b is characteristic of a Cu(II), $S = 1/2$ species rather than a corrole π cation radical, suggesting that the unpaired electron on the π system of one macrocycle of [(OEC²⁺)Cu^{II}(OEC^{•+})Cu^{II}] is coupled with the unpaired electron of one of the two Cu(II) ions. However, this ESR signal has an intensity lower than that in Figure 5a, thus suggesting that ~60% of the half-oxidized dimers may also exist in an $S = 3/2$ spin state, which is difficult to spectrally observe by ESR.²⁶

The removal of a second electron from [(OEC²⁺)Cu^{II}(OEC^{•+})Cu^{II}] then results in formation of [(OEC²⁺)Cu^{II}]₂. This species shows a well-defined $S = 1$ triplet spectrum as seen in Figure 5c and is formulated as a bis-Cu(II) complex having two doubly oxidized π ring systems.

[(OEC)Co]₂^{•+}. Neutral (OEC)Co is ESR silent. The ESR spectrum of [(OEC)Co]₂⁺ in frozen CH₂Cl₂ at 77 K, which was produced by exhaustive controlled-potential electrolysis of (OEC)Co at +0.4 V in CH₂Cl₂, 0.2 M TBAP, is shown in Figure 6. A similar spectrum can also be obtained in PhCN. The spectrum in Figure 6, which is typical of Co(II) ions,³⁴ shows a major line at $g_{\perp} = 2.40$ and a weak signal at $g_{\parallel} = 1.89$. The parallel component of this signal has well-resolved eight-line splitting due to the $I = 7/2$ ⁵⁹Co nucleus with $a = 62.5$ G.

The presence of a Co(II) ion in [(OEC)Co]₂²⁺ can be explained as discussed above for the (OEC)Cu derivative, the only difference being in the degree of interaction between the two singly oxidized (OEC)M units. [(OEC)Cu]₂²⁺ shows a triplet spectrum, but the doubly oxidized (OEC)Co dimer is ESR silent, which suggests that the two unpaired electrons of the two Co(II) ions in [(OEC)Co]₂²⁺ are coupled in PhCN. The doubly oxidized dimer is unstable in CH₂Cl₂ on the time scale of bulk electrolysis.

The addition of pyridine to PhCN solutions of [(OEC)Co]₂⁺ or [(OEC)Co]₂²⁺ results in the appearance of a strong $g = 2.00$ signal and, in the case of [(OEC)Co]₂⁺, in the complete disappearance of the signal at $g = 2.40$. A $g = 2.00$ signal could also be obtained by addition of Cl⁻ or imidazole to a solution of the singly or doubly oxidized cobalt dimers. The

(34) Walker, F. A. *J. Magn. Reson.* **1974**, *15*, 201.

(21) Fajer, J.; Borg, D. C.; Forman, A.; Dolphin, D.; Felton, R. H. *J. Am. Chem. Soc.* **1970**, *92*, 3451.

(22) Fuhrhop, J.-H.; Wasser, P.; Riesener, D.; Mauzerall, D. *J. Am. Chem. Soc.* **1972**, *94*, 7996.

(23) (a) Scheidt, W. R.; Cheng, B.; Haller, K. J.; Mislankar, A.; Rae, A. D.; Reddy, K. V.; Song, H.; Orosz, R. D.; Reed, C. A.; Cukiernik, F.; Marchon, J.-C. *J. Am. Chem. Soc.* **1993**, *115*, 1181. (b) Scheidt, W. R.; Brancato-Buentello, K. E.; Song, H.; Reddy, K. V.; Cheng, B. *Inorg. Chem.* **1996**, *35*, 7500. (c) Brancato-Buentello, K. E.; Kang, S.-J.; Scheidt, W. R. *J. Am. Chem. Soc.* **1997**, *119*, 2839.

(24) (a) Buchler, J. W.; Scharbert, B. *J. Am. Chem. Soc.* **1988**, *110*, 4272. (b) Buchler, J. W.; De Cian, A.; Fischer, J.; Hammerschmitt, P.; Weiss, R. *Chem. Ber.* **1991**, *124*, 1051. (c) Kadish, K. M.; Moninot, G.; Hu, Y.; Dubois, D.; Ibnlfassi, A.; Barbe, J.-M.; Guillard, R. *J. Am. Chem. Soc.* **1993**, *115*, 8153. (d) Guillard, R.; Barbe, J.-M.; Ibnlfassi, A.; Zrineh, A.; Adamian, V. A.; Kadish, K. M. *Inorg. Chem.* **1995**, *34*, 1472.

(25) See, for example: (a) Song, H.; Rath, N. P.; Reed, C. A.; Scheidt, W. R. *Inorg. Chem.* **1989**, *28*, 1839. (b) Song, H.; Orosz, R. D.; Reed, C. A.; Scheidt, W. R. *Inorg. Chem.* **1990**, *29*, 4274. (c) Scheidt, W. R.; Song, H.; Haller, K. J.; Safo, M. K.; Orosz, R. D.; Reed, C. A.; Debrunner, P. G.; Schulz, C. E. *Inorg. Chem.* **1992**, *31*, 939. (d) Schulz, C. E.; Song, H.; Lee, Y. J.; Mondal, J. U.; Mohanrao, K.; Reed, C. A.; Walker, F. A.; Scheidt, W. R. *J. Am. Chem. Soc.* **1994**, *116*, 7196.

(26) Godziela, G. M.; Goff, H. M. *J. Am. Chem. Soc.* **1986**, *108*, 2237.

(27) Lemtur, A.; Chakravorty, B. K.; Dhar, T. K.; Subramanian, J. *J. Phys. Chem.* **1984**, *88*, 5603.

(28) (a) Felton, R. H.; Owen, G. S.; Dolphin, D.; Fajer, J. *J. Am. Chem. Soc.* **1971**, *93*, 6332. (b) Chang, D.; Cocolios, P.; Wu, Y. T.; Kadish, K. M. *Inorg. Chem.* **1984**, *23*, 1629.

(29) Kadish, K. M.; Bolas, P.; D'Souza, F.; Aukauloo, M. A.; Guillard, R.; Lausmann, M.; Vogel, E. *Inorg. Chem.* **1994**, *33*, 471.

(30) Vogel, E.; Will, S.; Schulze Tilling, A.; Neumann, L.; Lex, J.; Bill, E.; Trautwein, A. X.; Wiegardt, K. *Angew. Chem., Int. Ed. Engl.* **1994**, *33*, 731; *Angew. Chem.* **1994**, *106*, 771.

(31) Will, S.; Lex, J.; Vogel, E.; Adamian, V. A.; Van Caemelbecke, E.; Kadish, K. M. *Inorg. Chem.* **1996**, *35*, 5577.

(32) Subramanian, J. In *Porphyrins and Metalloporphyrins*; Smith, K. M., Ed.; Elsevier: Amsterdam, 1975; p 555.

(33) (a) Mengersen, C.; Subramanian, J.; Fuhrhop, J.-H. *Mol. Phys.* **1976**, *32*, 893. (b) Eaton, S. S.; Eaton, G. R.; Chang, C. K. *J. Am. Chem. Soc.* **1985**, *107*, 3177.

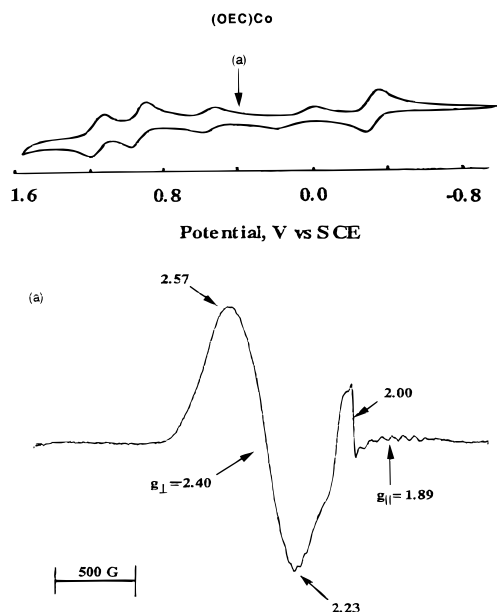


Figure 6. X-band EPR spectrum of $[(\text{OEC})\text{Co}]_2^+$ obtained in frozen CH_2Cl_2 solutions at 77 K (9.500 GHz, modulation 15 G) after bulk controlled-potential oxidation of (OEC)Co in CH_2Cl_2 at +0.4 V vs SCE.

Table 3. Half-Wave Potentials (V vs SCE) for Oxidation and Reduction of (OEC)Co in Solvents Containing 0.2 M TBAP

solvent	species in solution	oxidn				redn	
		4th	3rd	2nd	1st	1st	2nd
CH_2Cl_2	(OEC)Co	1.17	0.94	0.57	0.11	-0.30	-1.94 ^a
PhCN	(OEC)Co	1.38 ^a	0.86	0.49	0.14	-0.33	not obsd
PhCN + 0.08 M py	$(\text{OEC})\text{Co}(\text{py})_n$ ($n = 1$ or 2)				0.10	-0.55	-1.95

^a Irreversible process. Value listed is E_p at a scan rate of 0.1 V/s.

isotropic ESR spectrum at $g = 2.00$, $\Delta H = 45$ G with no detectable hyperfine splitting on the ^{59}Co nucleus is typical of cobalt(III) porphyrin π cation radicals.^{35–37} This would be the first clear example of a cobalt(III) corrole π cation radical. The only other known singly oxidized cobalt(III) corrole has been assigned as having a Co(IV) oxidation state on the basis of its ESR spectrum.¹² The appearance of a π cation radical signal after addition of py to the ESR-silent $[(\text{OEC})\text{Co}]_2^{2+}$ suggests that pyridine breaks the dimer with formation of $[(\text{OEC}^+\text{Co})\text{III}(\text{py})_n]$, where $n = 1$ or 2 . This result agrees with the electrochemical data for (OEC)Co in the presence of pyridine, where there is no evidence for formation of (OEC)Co dimers under these experimental conditions. For example, (OEC)Co in pyridine or PhCN/pyridine mixtures undergoes a well-defined single one-electron oxidation and two one-electron reductions (see Table 3), all three of which have the same maximum peak current. This is consistent with both the absence of dimer formation and literature data which show that (OEC)Co exists as either the mono- or bis-pyridine adduct in solutions containing pyridine.^{4,7,8}

In summary, the electrochemical and chemical reactions associated with the initial oxidations of (OEC)Co in CH_2Cl_2 , PhCN, and PhCN/py mixtures are proposed to occur as summarized in Scheme 1, where $[(\text{OEC})\text{Co}]_2^+$, $[(\text{OEC})\text{Co}]_2^{2+}$, and $[(\text{OEC})\text{Co}(\text{py})_n]^+$ represent three different oxidized forms of the corrole.

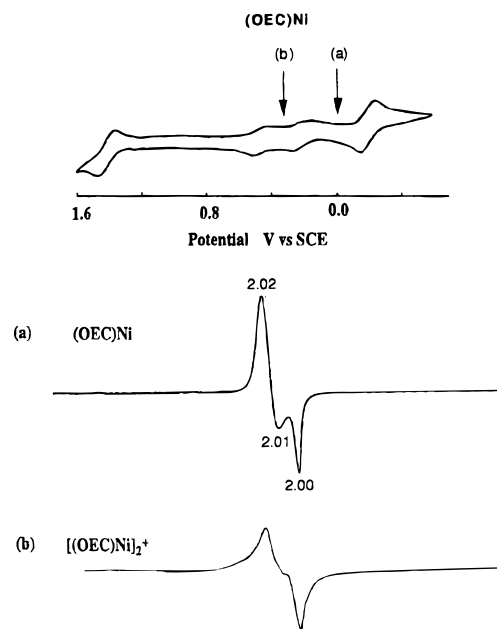
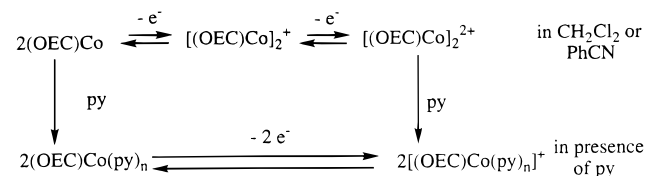


Figure 7. EPR signals of (a) (OEC)Ni and (b) $[(\text{OEC})\text{Ni}]_2^+$ in frozen CH_2Cl_2 solutions at 130 K after bulk controlled-potential electrolysis of (OEC)Ni in CH_2Cl_2 , 0.2 M TBAP. The applied potentials are shown with arrows in the cyclic voltammogram inset.

Scheme 1



(OEC)Ni and $[(\text{OEC})\text{Ni}]_2^{2+}$. The ESR spectrum of (OEC)Ni at 130 K in CH_2Cl_2 is shown in Figure 7a. The spectrum is similar to what has been previously reported in the literature for the same compound under slightly different experimental conditions¹⁴ and has been assigned to a Ni(II) π cation radical.

The bulk controlled-potential oxidation of (OEC)Ni at $E_{\text{app}} = +0.36$ V results in the formation of $[(\text{OEC})\text{Ni}]_2^+$ after a coulometric abstraction of 0.5 electron per molecule of the neutral compound, and this is accompanied by an approximately 50% decrease in intensity of the ESR signal (see Figure 7b). A further oxidation of the dimer at $E_{\text{app}} = +0.70$ V leads to $[(\text{OEC})\text{Ni}]_2^{2+}$, and this is accompanied by the complete disappearance of the ESR signal. These data again confirm the existence of oxidized Ni corrole dimers.

Nature of the Dimer. Porphyrin²⁵ and corrole¹⁸ π cation radicals are known to form strong π - π dimers in the solid state. There are also several examples in the literature for the formation in solution of oxidized porphyrin dimers containing nonelectroactive central metal ions and one²³ or two^{21–23,26} oxidized π ring systems. However, we know of only one example in the porphyrin literature where the formation of π - π dimers from monomers could be electrochemically detected.²⁷

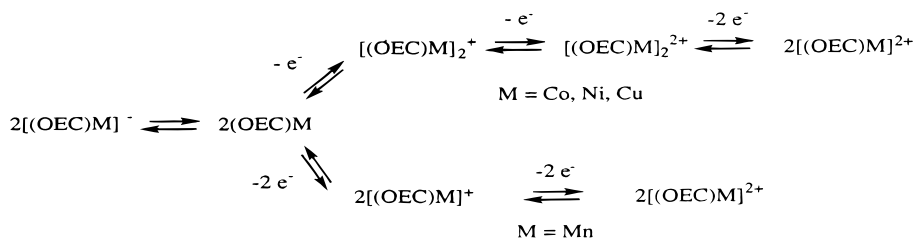
A strong interaction between electroactive redox centers is often observed upon oxidation of two tetrapyrrole macrocycles held together by a central bridging atom, with the most relevant examples being μ -oxo iron dimers^{28–30} and sandwich-type bisporphyrins with lanthanide or actinide central metal ions.²⁴ The magnitude of the interaction in such compounds depends on the distance between the two equivalent redox centers and can be related to the difference in $E_{1/2}$ between two consecutive

(35) Ichimori, K.; Ohya-Nishiguchi, H.; Hirota, N.; Yamamoto, K. *Bull. Chem. Soc. Jpn.* **1985**, 58, 623.

(36) Kadish, K. M.; Lin, X. Q.; Han, B. C. *Inorg. Chem.* **1987**, 26, 4161.

(37) Wolberg, A.; Manassen, J. *J. Am. Chem. Soc.* **1970**, 92, 2982.

Scheme 2



redox reactions.^{28,29} Specifically, if the two equivalent redox-active units do not interact, they will both be oxidized at the same potential. However, if an interaction exists between the two equivalent units, they will be oxidized at different potentials with the magnitude of the potential difference being larger for stronger interactions.

The experimentally measured difference in $E_{1/2}$ between two consecutive oxidations of μ -oxo iron dimers, $\Delta E_{1/2}$, ranges from 0.2 to 0.5 V for compounds having porphyrin²⁸ or porphycene²⁹ macrocycles. Sandwich-type bis-porphyrins also have $\Delta E_{1/2}$ values between 0.34 and 0.61 V, reflecting a strong interaction between the two macrocycles.²⁴ The $\Delta E_{1/2}$ between the two reversible oxidations of (OEC)M (actually, [(OEC)M]₂) in CH₂Cl₂ is 0.46 V for M = Co, 0.26 V for M = Ni, and 0.14 V for M = Cu, suggesting a stronger interaction in the case of the Co dimer than in the case of the Ni or Cu complex.

Electrooxidized (OEC)Co(C₆H₅)³¹ and (OEC)Fe(NO)^{18b} form π - π complexes in the solid state, where the two macrocyclic planes are separated by 4.13 and 3.96 Å, respectively. An even closer approach between the two macrocycles is seen in half-oxidized octaethylporphyrin dimers of the type [(OEP)M]₂⁺, where the average distance between the two metal centers in the mixed-valence dimers is 3.52 Å.^{23b} The distance between the two Cu centers in [(OEC)Cu]₂²⁺ was calculated as 3.88 Å from ESR data, as discussed in the previous section, and is larger than what has been calculated for the related [(OEP)M]₂⁺ π - π dimers. However, it should be noted that the two series of compounds differ in the total positive charge of the macrocycle. Specifically, the porphyrin π - π dimers, [(OEP)M]₂ⁿ⁺, contain

two M(II) metal ions and one ($n = 1$) or two ($n = 2$) positive charges over the two macrocycles while the corrole π - π dimers, [(OEC)M]₂ⁿ⁺, also contain two M(II) ions but have a positive charge of +3 ($n = 1$) or +4 ($n = 2$) over the two macrocycles.

Summary. Scheme 2 summarizes the two types of electrochemical behavior which are observed for the investigated (OEC)M complexes.

The oxidation of (OEC)Co, (OEC)Ni, and (OEC)Cu, which all exist as monomeric species, occurs via formation of dimeric species, and this is in contrast to the case of (OEC)Mn, which exists only as a monomer in both its neutral and oxidized forms. Dimeric [(OEC)M]₂⁺ and [(OEC)M]₂²⁺ unequivocally contain metal ions in a +2 oxidation state when M = Cu or Co, and a similar oxidation state assignment may be assumed in the case of [(OEC)Ni]₂⁺ and [(OEC)Ni]₂²⁺. Neither dimers nor π cation radicals are formed after the first electrooxidation of (OEC)-Mn, where a Mn(IV) corrole is clearly electrogenerated. We believe that the site of electron transfer in (OEC)Mn is the reason for the absence of dimerization, and this is consistent with data now in the literature for related mixed-valent π - π octaethylporphyrin dimers, all of which contain oxidized macrocycles.

Acknowledgment. The support of the Robert A. Welch Foundation (K.M.K., Grant E-680) is gratefully acknowledged. We also thank Dr. Vadim Kourshev for the help with ESR experiments at 77 K and Dr. Marie Autret for electrochemical measurements on (OEC)Mn.

JA9814570